



Ciencia e Ingeniería Neogranadina

ISSN: 0124-8170

ISSN: 1909-7735

Universidad Militar Nueva Granada

Benjumea, José M.; Chio Cho, Gustavo; Fernández W., Angélica; Ardila, Javier A.  
Acceleration Amplitude of the Vertical Component of Colombian Earthquakes\*  
Ciencia e Ingeniería Neogranadina, vol. 32, no. 1, 2022, January-June, pp. 83-97  
Universidad Militar Nueva Granada

DOI: <https://doi.org/10.14482/INDES.30.1.303.661>

Available in: <https://www.redalyc.org/articulo.oa?id=91172083007>

- How to cite
- Complete issue
- More information about this article
- Journal's webpage in redalyc.org

UDEM  redalyc.org

Scientific Information System Redalyc  
Network of Scientific Journals from Latin America and the Caribbean, Spain and  
Portugal

Project academic non-profit, developed under the open access initiative



# Acceleration Amplitude of the Vertical Component of Colombian Earthquakes\*

José M. Benjumea<sup>a</sup> ■ Gustavo Chio Cho<sup>b</sup> ■ Angélica Fernández W.<sup>c</sup> ■  
Javier A. Ardila<sup>d</sup>

**Abstract:** Past studies have demonstrated that the vertical earthquake component can substantially affect the seismic performance of bridges and buildings. This component is typically ignored or, when included in the design, is estimated as two-thirds of the horizontal seismic design earthquake. This paper presents the characterization of the acceleration amplitude of the vertical component of moderate and strong earthquakes in Colombia (Moment magnitude  $M_w > 4$ ) that occurred between June 1993 and April 2020. A total of 42 seismic records registered at less than 50 km from the rupture plane and with horizontal acceleration peaks greater than 0.05g were selected. The peak ground acceleration (PGA) of the three components and the ratio between those PGAs were calculated. Additionally, the relationship among those parameters and the magnitude and epicentral and hypocentral distances were determined. The results showed that the V/H ratio equal to 2/3 is not always valid to represent the effects of the vertical component in structures subjected to the moderate and strong ground motions in Colombia.

**Keywords:** Hypocentral distance; V/H ratio; V/H spectral ratio; peak ground acceleration (PGA); vertical ground motion

**Recibido:** 05/06/21 **Aceptado:** 29/11/2021

**Disponible en línea:** 03/06/2022

**Cómo citar:** J. M. Benjumea, G. Chio Cho, A. Fernández W., and J. A. Ardila, "Acceleration Amplitude of the Vertical Component of Colombian Earthquakes", *Cien.Ing.Neogranadina*, vol. 32, no. 1, pp. 87-101, Jun 2022.

\* Research paper.

**a** PhD. in Civil and Environmental Engineering. Associate Professor, Civil Engineering School, Universidad Industrial de Santander, Bucaramanga, Colombia. E-mail: josbenro@uis.edu.co  
ORCID: <http://orcid.org/0000-0001-5654-948X>

**b** PhD. in Road, Channel, and Port Engineering. Full professor, Civil Engineering School, Universidad Industrial de Santander, Bucaramanga, Colombia. E-mail: gchioch@uis.edu.co  
ORCID: <http://orcid.org/0000-0003-4766-9759>

**c** BS Civil Engineering. Universidad Industrial de Santander, Bucaramanga, Colombia.  
E-mail: maria.fernandez6@correo.uis.edu.co ORCID: <http://orcid.org/0000-0002-1692-7519>

**d** BS Civil Engineering. Universidad Industrial de Santander, Bucaramanga, Colombia.  
E-mail: javier.ardila3@correo.uis.edu.co ORCID: <http://orcid.org/0000-0002-7759-5327>

## *Amplitud de aceleración del componente vertical de los sismos colombianos*

**Resumen:** Estudios anteriores han demostrado que el componente vertical del terremoto puede afectar sustancialmente el desempeño sísmico de puentes y edificios. Este componente generalmente se ignora o, cuando se incluye en el diseño, se estima como dos tercios del terremoto de diseño sísmico horizontal. Este trabajo presenta la caracterización de la amplitud de aceleración del componente vertical de sismos moderados y fuertes en Colombia (Magnitud de momento  $M_w > 4$ ) ocurridos entre junio de 1993 y abril de 2020. Se registraron un total de 42 registros sísmicos a menos de 50 km del Se seleccionaron planos de ruptura y con picos de aceleración horizontal mayores a 0.05g. Se calcularon la aceleración máxima del suelo (PGA) de los tres componentes y la relación entre esos PGA. Adicionalmente, se determinó la relación entre dichos parámetros y la magnitud y las distancias epicentral e hipo central. Los resultados mostraron que la relación V/H igual a 2/3 no siempre es válida para representar los efectos del componente vertical en estructuras sometidas a movimientos de suelo moderados y fuertes en Colombia.

**Palabras clave:** distancia hipo central; relación V/H; relación espectral V/H; aceleración máxima del suelo (PGA); movimiento vertical del suelo

## Introduction

Traditionally, the seismic damage in buildings and infrastructure systems has been associated with the horizontal components of ground motions. Nonetheless, reconnaissance reports after major earthquakes like Loma Pieta (USA, 1989,  $M_w = 6.9$ ), Kobe (Japan, 1995,  $M_w = 6.9$ ), and L'Aquila (Italy, 2009,  $M_w = 6.1$ ) showed that the vertical earthquake component can generate significant damage to structural and non-structural elements. The damage caused by the vertical motions is attributed to substantial variations in the axial forces and the associated reduction of the shear resistance in vertical members like columns or walls, and to significant amplification of bending moments and shear forces in beams and girders [1]–[4]. The extent of those magnifications depends on the structural system and the characteristics of the ground motion. The latter are generally referred to as seismic intensity parameters and lie within three categories: amplitude, duration, and spectral responses [5], [6].

The main acceleration amplitude characteristics for the ground motions are the vertical peak ground acceleration ( $PGA_V$ ) and the V/H ratio, which is the ratio between  $PGA_V$  and the  $PGA$  of the horizontal components. Past studies developed in seismotectonic environments different than Colombia have demonstrated that the  $PGA_V$  and V/H ratios depend on the magnitude of the seismic event, site conditions, source-to-site distance, fault mechanism, among others [7]–[10]. The V/H ratios are larger than 1.0 and 2/3 for source-to-site distances lesser than 5 km and 25 km, respectively ([7], [10]) and seem to be weakly related to the earthquake magnitude and faulting mechanism but highly influenced by the local site conditions [9].

The factors mentioned above suggest that structural systems should be designed to include the effects of the vertical ground motions, especially for near-fault locations. Despite this, insufficient attention is given to the vertical earthquake component in the Colombian codes for the design of buildings (NSR-10 [11]) and bridges (CCP-14 [12]). For example, Section A.2.8 of the NSR-10 Code

indicates that the minimum vertical seismic design motion may be taken as two-thirds of the horizontal design motion, being the latter represented by a pseudo-acceleration response spectrum or a family of accelerograms. The V/H ratio equal to 2/3 is a rule-of-thumb that has been adopted in practice after that ratio was proposed by Newmark et al. [13] using data from 33 earthquake records in California, USA.

This study focuses on characterizing the acceleration amplitude parameters,  $PGA_V$  and the V/H ratio, of the moderate-to-strong ground motions in Colombia recorded between June 1993 and April 2020. These intensity parameters were correlated to the moment magnitude and epicentral and hypocentral distances of the events to determine potential relationships among the parameters. In light of the results, the adequacy of the minimum V/H ratio equal to 2/3 recommended in NSR-10 is assessed.

## Materials and methods

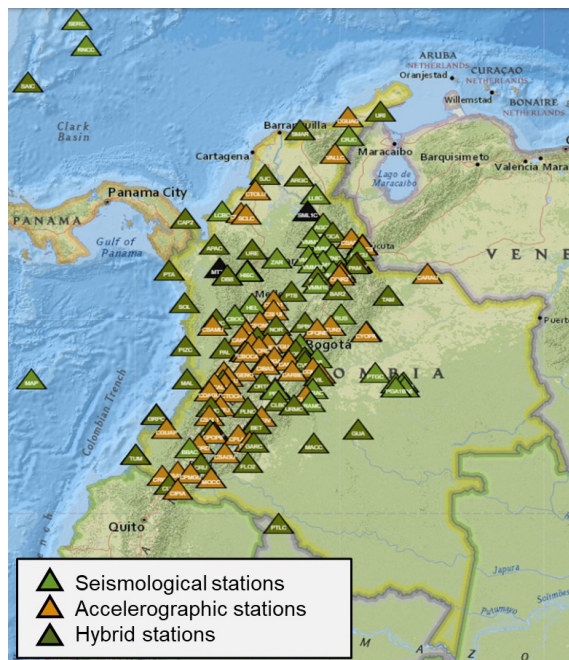
This section describes the main steps in the selection and pre- and post-processing of the earthquake records. The seismic intensity parameters and the steps used to determine their relationship are also described.

### Selection and processing of ground motion records

The Servicio Geológico Colombiano (SGC) monitors the seismic activity in Colombia through the national accelerograph seismic network. As of April 2021, the network consisted of 176 active stations (Fig. 1): 88 with an accelerometer only, 38 with a seismometer, and 50 hybrid accelerometer-seismometers sensors [14]. The accelerations records from those stations are compiled in two seismic catalogs available at [15]. For the interested reader, the characteristics of each station, including its location, elevation, topographic condition, and type of sensor and instrumental response, can be obtained by clicking on the station of interest in the map provided by [14]. The first catalog contains the acceleration records of the seismic events

between June 1, 1993, and December 31, 2017. The second catalog contains the records of the events that have occurred since January 1, 2008. A negative aspect of the available information in the SGC database is that the local soil conditions of the stations are not detailed. Thus, instead of categorizing the soil profiles within any of the typical A to E profiles (based on the average shear wave velocity of the upper 30 m), only a basic classification like “rock,” “soil,” “soil-rock,” is provided. Moreover, the faulting mechanism of each seismic event is not reported.

**Fig. 1.** Distribution of seismic stations in Colombia.



**Source:** Servicio Geológico Colombiano [14].

The initial and final dates used for selecting the seismic events investigated in this paper were June 1, 1993, and April 30, 2020, respectively, covering approximately 27 years. The selection criteria for the seismic events and ground motion records comprised three conditions. First, a minimum moment magnitude ( $M_w$ ) of the events of 4.0 was set to guarantee that only moderate and strong earthquakes were included in the analysis. Second, the maximum epicentral distance ( $R_{epic}$ ) between the epicenter and the seismic station was set to 50 km. This threshold was selected because the vertical earthquake

component is more relevant for near-site locations. Last, a minimum peak ground acceleration (PGA) of any of the two horizontal components of the records of 0.05 g was set, where g is the acceleration due to gravity. This criterium was applied to avoid the inclusion of noise-like recordings that could lead to unrepresentative V/H ratios. The 0.05 g umbral coincides with the acceleration threshold used to determine the absolute bracketed duration [16]. No limit was imposed to the hypocentral distance ( $R_{hypo}$ ) to avoid significant reduction of the dataset and evaluate the depth effect on the acceleration amplitude of the vertical motions.

Each record has three acceleration signals, two for the horizontal components and one for vertical. The signals were pre-and post-processed using a script developed by the authors in the software Matlab [17]. Instrumental correction was not applied to the records because the SGC website [15] states that such correction had already been performed. The accuracy of the Matlab script was determined by calculating several seismic intensity parameters for the Loma Prieta earthquake records at Gilroy Arrays #1 and #2 and comparing them to those determined using the commercial software SeismoSignal [18], and those reported [19]. The largest difference obtained was 6.5%, indicating that the script was satisfactory. Further verifications performed for two earthquake records from the Córdoba, Quindío, 1999 earthquake (event #4 in Table 1) resulted in differences less than 1%. The comparisons are available at [20], while the script can be downloaded from [21].

The basic steps performed by the Matlab script are as follows. First, the acceleration data from the SGC files (in ANC format) are read. Then, the velocity and displacement of each component are calculated by single and double integration of the acceleration, respectively. A cubic-polynomial baseline correction is then applied to the acceleration histories using the command “detrend.” Subsequently, the Fourier spectra of the acceleration histories of each component are plotted to determine potential spurious frequency content such as noise that should be dampened or removed. When needed, a 0.2-50 Hz bandpass Butterworth filter was applied to the acceleration

signal. The Fourier spectra and the acceleration, velocity, and displacement traces are then plotted to compare the original and processed data to confirm that the main characteristics of the original record had not been removed. The processed records are then used to determine the seismic intensity parameters described next.

## Seismic intensity parameters

The parameters used to characterize the acceleration amplitude of the vertical earthquake motions in Colombia are the  $PGA$ , the  $V/H$  ratio, and  $V/H_{GM}$ . The  $V/H$  ratio was determined separately for each of the two horizontal components, while the  $V/H_{GM}$  ratio was introduced to obtain a general relationship between the vertical and the horizontal motions. For this parameter, the geometric mean (GM) of the  $PGA$  of the horizontal components was selected to describe the overall horizontal motion. The geometric mean is an output of ground motion prediction equations [22] and is an intensity measure used to perform probabilistic structural response analyses [23]. Subscripts “V,” “EW,” and “NS” are used in this paper to differentiate the parameters for the vertical and the two horizontal components (East-West and North-South), respectively.

## Relationships among parameters and regression analyses

The relationships among the  $PGAs$  and the  $V/H$  ratios and the magnitude ( $M_w$ ), epicentral distance ( $R_{epic}$ ), and hypocentral distance ( $R_{hypo}$ ) were determined through the Pearson correlation coefficient ( $r_{XY}$ ). This coefficient measures the linear dependency between two random variables  $X$  and  $Y$ , and is calculated using (1), in which  $\bar{X}$  and  $\bar{Y}$  are the mean of the two variables. The Pearson correlation coefficient ranges between -1 and 1, with the two extremes indicating direct positive and negative linear correlations, respectively. An  $r_{XY} = 0$  indicates no linear correlation between the two variables, although this does not mean that the variables are independent. In this paper, the linear relationship between two parameters was regarded as strong when  $|r_{XY}| \geq 0.8$ , moderate when  $0.5 \leq |r_{XY}| < 0.8$ , and weak if  $|r_{XY}| < 0.5$ . The

statistical significance of the linear correlation was calculated through p-values to test the null hypothesis that no linear relationship existed. The null hypothesis was therefore rejected when the p-value was smaller than 0.05. The correlation coefficient and the p-value were calculated using the open-source software R [24].

$$r_{XY} = \frac{\sum (X - \bar{X})(Y - \bar{Y})}{\sqrt{\sum (X - \bar{X})^2 \sum (Y - \bar{Y})^2}} \quad (1)$$

The Pearson coefficients were assembled in a cross-correlation matrix to visualize the relationships among the parameters. The cross-correlation matrix was determined and plotted using the software R [24] and the library “Performance Analytics” developed by [25]. Then, multivariate regression analyses were performed to propose simplified equations that predict the  $PGA_V$  and  $V/H$  ratios. The models were based on the results of the cross-correlation analysis and the models proposed by other authors. Significance levels of the coefficients associated with the predictor variables were calculated to assess if any of the predictors could be removed. Lastly, the determination coefficient ( $R^2$ ) and significance level of the models were calculated. The models and their significance levels were determined using the function “lm” (fitting linear models) available in the software R. Library “ggplot2”, developed by [26], was used to plot the correlation between the models and the measured data.

## Results

### Selected ground motions

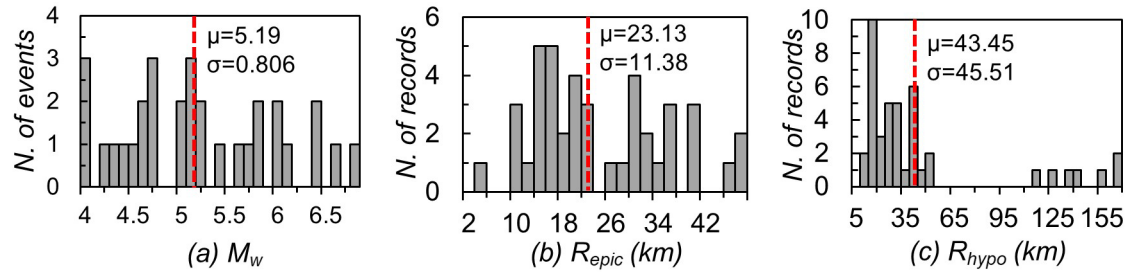
Table 1 lists the resulting seismic events (31) and associated records (42) after applying the selection criteria discussed in the previous section. The relatively low ratio between the number of records and seismic events (equal to 1.375) suggests a shortage of seismic stations located in sites near active sources. Despite the continuous addition of seismic stations in the last few years by the SGC, further efforts are still needed to enhance the Colombian seismic network.



Fig. 2 shows the frequency distributions for the magnitude and the epicentral and hypocentral distances of the earthquake records. Also shown in the plots are the mean value ( $\mu$ ), marked as a dashed line, and the standard deviation ( $\sigma$ ). The 31 seismic events have moment magnitudes ranging between 4.0 and 6.8, and their mean and mode are 5.19 and 5.10 (three events),

respectively. Most of the records correspond to epicentral distances smaller than 27 km (25/42), and the closest and farthest distances among all cases were 3 km and 47.44 km, respectively. The hypocentral distances ( $R_{hypo}$ ) are shallower than 50 km in 35 out of the 42 records, meaning that most of the records are superficial or have intermediate depth.

**Fig. 2.** Frequency distribution of (a) earthquake magnitude and (b) epicentral and (c) hypocentral distances.



**Source:** The authors.

**Table 1.** Selected events and records.

Event #	Date (M/D/Y)	$M_w$	Epicenter	Station	Soil Type	$R_{epic}$ (km)	$R_{hypo}$ (km)
1	02/08/1995	6.8	Calima, Valle del Cauca	CTRUJ	Rock	47.44	112.49
2	08/19/1995	6.6	Risaralda, Caldas	CANSE	Rock	18.43	122.30
1	07/18/1998	4.6	Ricaurte, Nariño	CRICA	Soil	13.70	13.70
4	01/25/1999	6.2	Córdoba, Quindío	CCAST	Soil	39.20	39.20
				CARME	Soil	13.02	13.02
				CFLAN	Soil	28.85	28.85
				CBOCA	Rock	38.48	38.48
5	06/01/1999	5.1	El Calvario, Meta	CVIL1	Rock	17.27	17.28
6	03/08/2005	5.1	Toro, Valle del Cauca	CVERS	Soil	13.77	14.65
				CPOST		47.13	47.39
				CPOST		14.31	14.41
7	06/22/2005	4	Córdoba, Quindío	CCALA	Rock	12.48	12.60
				CARME	Soil	14.31	14.41
8	11/25/2006	4.7	Ricaurte, Nariño	CSAMA	Rock	29.04	29.32
9	05/24/2008	4	Fómeque, Cundinamarca	CQUET	Rock	12.60	13.22
				CQUET	Rock	9.57	9.58
10	05/24/2008	5.6	Quetame, Cundinamarca	CBOG2	Soil	35.35	35.35
				CVIL1	Rock	31.66	31.66

Event #	Date (M/D/Y)	$M_w$	Epicenter	Station	Soil Type	$R_{epic}$ (km)	$R_{hypo}$ (km)
11	05/24/2008	4.4	Fómeque, Cundinamarca	CQUET	Rock	10.94	12.63
12	05/24/2008	4.3	El Calvario, Meta	CQUET	Rock	14.67	20.28
13	05/24/2008	4	El Calvario, Meta	CQUET	Rock	16.04	18.85
14	05/25/2008	4.2	Quetame, Cundinamarca	CQUET	Rock	9.21	10.04
15	09/13/2008	5.2	Palestina, Caldas	CPER2	Soil	20.58	138.93
16	12/18/2009	5.2	Caloto, Cauca	CPTJ	Soil	19.86	152.50
17	10/29/2014	4.6	Cumbal, Nariño	CCUMB	Rock	20.45	20.45
18	03/10/2015	6.4	Los Santos, Santander	CGIR2	Rock	20.89	161.36
				CBUCF	Rock	27.65	162.37
19	10/12/2015	4.7	Juradó, Chocó	CPTAR	Rock	45.14	45.35
20	02/06/2017	5.4	Colombia, Huila	CCOLO	Soil	9.24	9.24
21	08/18/2018	5.8	Mar Caribe	CAP2	Rock	3	14
22	10/04/2018	5.1	Mar Caribe	PRV	Rock	28	29
23	10/29/2018	5	Mar Caribe	CAP2	Rock	15	21
24	11/23/2018	4.5	Océano Pacífico	PTA	Rock	38	39
25	11/25/2018	6	Mar Caribe	PRV	Rock	24	28
26	11/25/2018	5.7	Mar Caribe	PRV	Rock	29	29
27	03/23/2019	6.1	Versalles, Valle del Cauca	PAL	Rock	31	130
28	05/24/2019	5	Juradó, Chocó	PTA	Rock	34	42
29	12/24/2019	6	Mesetas, Meta	CLEJA	Soil	18	22
				URMC	Soil	32	35
30	12/24/2019	5.8	Mesetas, Meta	CLEJA	Soil	15	19
				URMC	Soil	35	37
31	12/25/2019	4.7	Mesetas, Meta	CLEJA	Soil	18	20

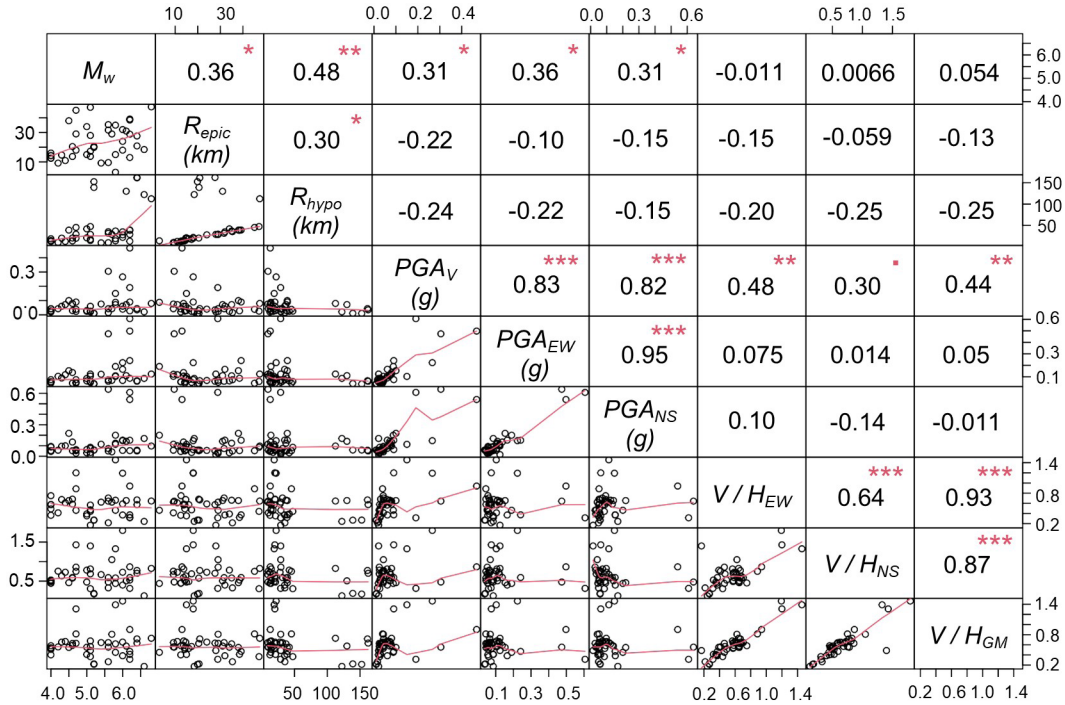
Source: Servicio Geológico Colombiano [15].

## Correlation among parameters

Fig. 3 shows the cross-correlation matrix for the seismic intensity parameters and the earthquake measurements  $M_w$ ,  $R_{epic}$ , and  $R_{hypo}$ . Each of these variables occupies the diagonal of the matrix. The upper triangular section of the matrix shows the Pearson correlation coefficient between two parameters. For example, the Pearson coefficient between  $M_w$  and  $PGA_V$  should be read at the position  $i = 1, j = 4$  in the upper triangular section ( $r_{1,4} = 0.31$ ). The symbols on top of the coefficient

indicate that the p-value lies in the following ranges: “\*\*\*” for range [0, 0.001]; “\*\*” for (0.001 to 0.01]; “\*” for (0.01 to 0.05]; and “.” for (0.05 to 0.1]. A coefficient without a symbol means that the p-value is in the range (0.1 and 1.0]. For the example, the associated p-value is in the range (0.05 to 0.10). The lower triangular section of the matrix shows the relationship between two parameters and a segmented mean line that helps visualize whether a linear relationship between the two parameters is appropriate.



**Fig. 3.** Visualization of cross-correlation matrix.

**Source:** The authors.

Fig. 3 shows that the  $PGA_V$  increases with the magnitude of the ground motion and decreases with epicentral and hypocentral distances. These trends coincide with those reported by other authors using data from other seismotectonic environments. The relatively low values (less than 0.31) of the Pearson coefficients for the pairs  $PGA_V-M_w$ ,  $PGA_V-R_{epic}$ , and  $PGA_V-R_{hypo}$  suggest that attenuation equations for the  $PGA_V$  should involve non-linear relationships among those parameters. The  $PGA$  of the horizontal components also exhibited a weak linear correlation with  $M_w$ ,  $R_{epic}$ , and  $R_{hypo}$ . However, the relationship between the horizontal  $PGAS$  and  $M_w$  is slightly stronger than that observed for the vertical component. Fig. 3 shows a strong linear relationship between  $PGA_V$  and the peak ground accelerations of the horizontal components. The Pearson coefficients for the pairs  $PGA_V-PGA_{EW}$  and  $PGA_V-PGA_{NS}$  are  $r_{4,5} = 0.83$  and  $r_{4,6} = 0.82$ , and the p-values of these relationships are smaller than 0.001, validating their linear relationship.

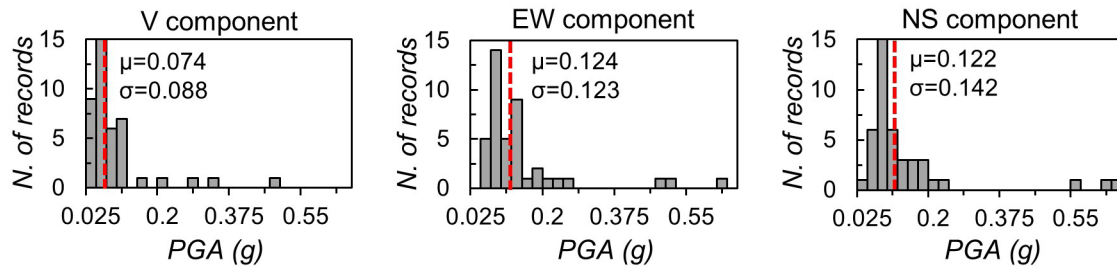
The linear correlation of the  $V/H$  ratios, including  $V/H_{GM}$ , with the earthquake measurements is significantly low, especially with  $M_w$ . This result agrees with the findings reported by [9]. The Pearson coefficients for the  $V/H-R_{epic}$  pair, which are smaller than  $|-0.13|$ , do not indicate that these variables are not correlated but that their linear correlation is low. For a dataset of 113 near-field and shallow worldwide earthquakes records, [8] also found that the linear relationship between the  $V/H$  ratio and  $R_{epic}$  was not strong. The  $V/H$  ratios of the records studied in this paper showed larger Pearson coefficients with the hypocentral distance, although they were smaller than  $|-0.25|$ . The negative value of the coefficient signifies that the  $V/H$  ratios decrease as  $R_{hypo}$  increases. The slightly larger correlation coefficients for the pair  $V/H-R_{hypo}$  mean that the rupture plane depth ( $h$ ) also influences the amplitude of the vertical earthquake motions (recall that both  $h$  and  $R_{epic}$  are used to calculate  $R_{hypo}$ ).

## Vertical peak ground acceleration

Frequency distribution plots for the  $PGA_V$  of the three components of the records studied in this paper are shown in Fig. 4. The mean  $PGA_V$  is 0.074g, while the three highest  $PGA_V$  values are 0.47g, 0.30g, and 0.27g, measured during events #4 (at CARME station), #10 (CQUET), and #29 (CLEJA), respectively. These three records are “near-site” records as their  $R_{epic}$  was equal to or smaller than 18 km. Fig. 4 shows that the PGAs of the three components seem to have a Gaussian distribution and that they are biased towards the lower values. A

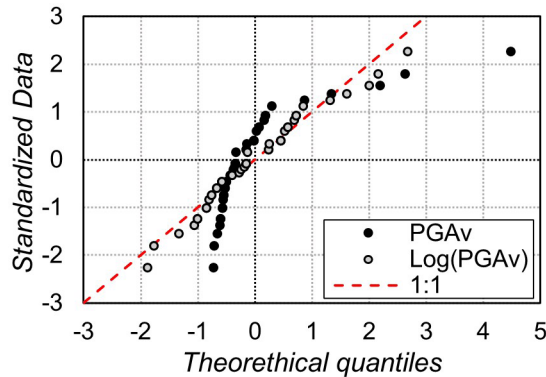
closer look at the  $PGA_V$  values showed that this data is not normally distributed, but its logarithmic transformation is. This was verified by plotting Quantile-Quantile plots, also known as Q-Q plots, which usually compare distributed independent data versus the standardized data of interest. The resulting Q-Q plots for the  $PGA_V$  and  $\log(PGA_V)$  are shown in Fig. 5. Note that the latter is closer to the line with a 1:1 slope, indicating that it fits better to a normal distribution. Similar results were obtained for the PGA of the two horizontal components but are not shown in the paper due to space constraints.

**Fig. 4.** Frequency distribution plots for the PGA of the three components.



**Source:** The authors.

**Fig. 5.** Q-Q plots for  $PGA_V$  and  $\log(PGA_V)$ .



**Source:** The authors.

The result described above was utilized to determine a model that describes  $PGA_V$  as a function of  $M_w$ ,  $R_{epi}$ , or  $R_{hypo}$ . Equ. (2) provides the overall form of the prediction model used in this study. This model is based on that by [8], but the last term

was added in this study because the  $PGA_V$  showed a slightly better correlation with  $R_{hypo}$ . Therefore, this predictor variable was also investigated. In their prediction model, [8] introduced the term  $h_o$  to account that the source of the peak motion is not necessarily the closest point on the projection surface of the fault. Nonetheless,  $h_o$  was not intended to incorporate the effect of the depth on the  $PGA_V$ . In this study,  $h_o$  was varied from 0.0 to 10 km every 0.5 km, which is similar to the range used by [8]. The resulting relationships were not intended to be proposed as attenuation models for implementation in seismic hazard analysis. This statement is especially true given the relatively small number of earthquake data that was used. Thus, the obtained models can be improved in the future as the dataset is enlarged.

$$\log(PGA_V) = C_1 + C_2 M_w + C_3 \log \left( \sqrt{R_{epic}^2 + h_o^2} \right) + C_4 \log(R_{hypo}) \quad (2)$$

The resulting coefficients ( $C_1$  to  $C_4$ ), determination coefficients ( $R^2$ ), and p-values for six different models are listed in Table 2. Asterisks (\*) are used again to indicate the significance range level of each coefficient. The ranges are the same as those used to describe Fig. 3. A dash (-) in Table 2 denotes that the variable was not included in the model.

The first three models show the effect of  $R_{epic}$  and  $h_o$ , with models 1 and 3 respectively corresponding to the upper and lower limits of  $h_o$ , with model 2 with the largest  $R^2$  value for  $h_o$ . These three models show that the intercept ( $C_1$ ) and  $M_w$  were more statistically significant in describing the variation of  $\log(PGA_V)$ . The marks “\*\*\*” correspond to a significance level range of [0, 0.001], whereas “\*” corresponds to (0.01 to 0.05).  $R_{epic}$ ,  $h_o$ , and  $R_{hypo}$  were

then integrated into the next model. After varying  $h_o$ , the largest determination coefficient of the new model set occurred when  $h_o = 0.0$  km (model 4). Although  $R^2$  in model 4 was larger than that in models 1 to 3, the low significance level of coefficient  $C_3$  indicates that the increment was mainly due to variable  $R_{hypo}$ . Model 4 was indeed rejected despite the larger  $R^2$  obtained because the positive value of  $C_3$  was not realistic (e.g., the  $PGA_V$  is expected to be smaller with a larger  $R_{epic}$ ). Accordingly, variables  $R_{epic}$  and  $h_o$  were removed, resulting in model 5. This model showed high statistically significant coefficients for the predictor variables and the largest determination coefficient of all the models ( $R^2$  close to 0.5). The overall improvement resulted from the moderate relationship observed for the pair  $PGA_V$ - $R_{hypo}$ , discussed above.

**Table 2.** Resulting coefficients for the prediction models.

Model	C1	C2	C3	$h_o$ (km)	C4	R2	p-value
1	-3.675***	0.420*	-0.518*	0.0	-	0.1563	0.01370
2	-3.388**	0.441**	-0.637*	5.5	-	0.1635	0.01168
3	-3.084**	0.446**	-0.727*	10.0	-	0.1600	0.01259
4	-4.262***	0.714***	0.0161	0.0	-0.745***	0.4352	1.62x10 <sup>-5</sup>
5	-4.265***	0.714***	-	-	-0.745***	0.4496	3.31x10 <sup>-6</sup>

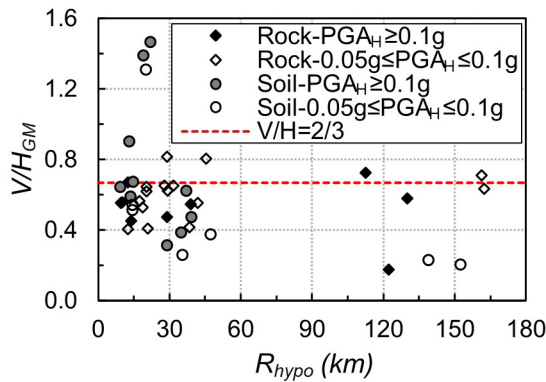
**Source:** The authors.

## V/H ratios

As shown in Fig. 4, the mean PGA of the vertical component is smaller than that of each horizontal component. The V/H ratios between those means are 0.574 ( $V/H_{EW}$ ) and 0.658 ( $V/H_{NS}$ ). These values are close to that adopted in NSR-10 as a minimum ( $V/H = 2/3$ ). However, their standard deviations ( $\sigma = 0.263$  for  $V/H_{EW}$  and  $\sigma = 0.337$  for  $V/H_{NS}$ ) are approximately 50% of the mean, exposing a relatively large variation. The dispersion can be observed in Fig. 6, in which the V/H ratios are plotted versus  $R_{hypo}$ . Note that different markers are used in that figure to differentiate the soil profile (either soil or

rock) and the intensity of the horizontal motion. For the latter, the motions were categorized in two ranges,  $0.05g \leq PGA_H < 0.1g$  and  $PGA_H \geq 0.1g$ , where  $PGA_H$  is the largest between  $PGA_{NS}$  and  $PGA_{EW}$  for a given record. The V/H ratios were larger than 2/3 in ten records, corresponding to approximately 24% of the cases. Moreover, the earthquake motions with V/H larger than 2/3 correspond to  $R_{hypo}$  shallower than 30 km (70% of the cases) and epicentral distances smaller than 21 km (70% of the cases). The soil profile effects were not evident in these records as half of them corresponded to rock sites and the remaining to soil sites.

**Fig. 6.** V/H ratio versus hypocentral distance for the 42 records.



Source: The authors.

Linear regression analyses were used to determine simple prediction equations for  $PGA_V$  as a function of  $PGA_{EW}$ ,  $PGA_{NS}$ , and  $PGA_{GM}$ . These equations can estimate the intensity of the vertical movements in cases where the accelerometer is biaxial or uniaxial (or even when it is triaxial, but one or two channels are damaged). The resulting relationships and determination coefficients ( $R^2$ ) are presented in (3) to (5). All p-values of the prediction models were smaller than  $2.2 \times 10^{-16}$ , meaning that they are statistically significant. The  $R^2$  and p-values indicate that those equations explain approximately 80 % of the variance of the  $PGA_V$  with a 95 % confidence level.

The reason why the coefficients of the predictor variables in (3) to (5) are close to each other can be explained by two factors. First,  $PGA_{EW}$  and  $PGA_{NS}$  have a strong linear correlation (Fig. 3) and their mean ratio is close to one ( $\mu = 0.98$ ,  $\sigma = 0.35$ ). Second, the difference between the mean  $V/H_{EW}$  (0.567) and the mean  $V/H_{NS}$  (0.658) is statistically insignificant. The latter was validated by performing a t-test for the differences between the means of the two ratios (p-value = 0.0614) and an F-test for the difference in the variances (p-value = 0.519). The null hypothesis of both tests is that no significant difference existed; hence, the p-values larger than 0.05 mean that the null hypothesis cannot be rejected. Fig. 7 shows the relationship between the measured  $PGA_V$  and  $PGA_{GM}$  and that resulting from (5) along with the 95 %-confidence region. The more considerable differences between

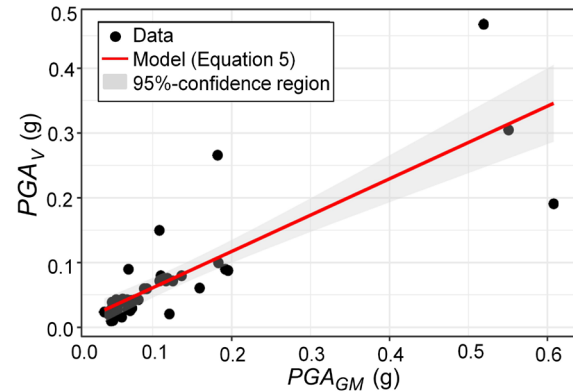
the predicted and measured data occur as the intensity of the vertical ground motion increases, which corresponds to larger amplitudes of the horizontal motions.

$$PGA_V = 0.593 PGA_{EW}, (R^2 = 0.814) \quad (3)$$

$$PGA_V = 0.549 PGA_{NS}, (R^2 = 0.797) \quad (4)$$

$$PGA_V = 0.583 PGA_{GM}, (R^2 = 0.817) \quad (5)$$

**Fig. 7.** Measured and predicted relationships between  $PGA_V$  and  $PGA_{GM}$ .



Source: The authors.

The mean V/H ratios and the coefficients of the prediction models are close to the  $V/H = 2/3$  suggested in NSR-10 as a minimum ratio to construct the vertical acceleration design spectrum based on the horizontal design spectrum. This closeness could indicate that the recommendation in NSR-10 is sufficient to construct the entire vertical acceleration design spectrum. However, as discussed next, a single value for the V/H ratio may not be adequate.

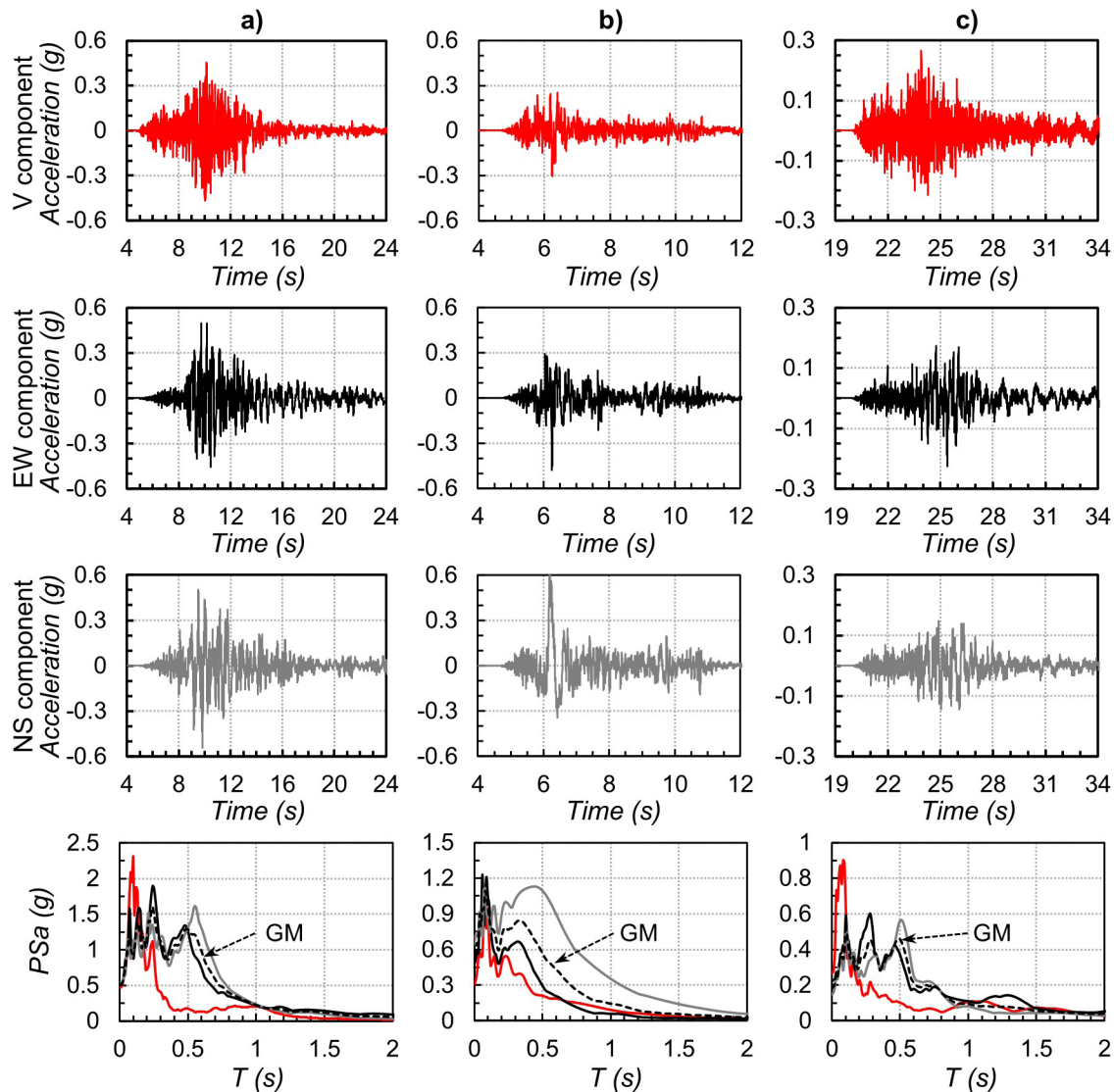
Three earthquake records were selected as examples to demonstrate the issue mentioned above. The records correspond to ground motions #4, #10, and #29, recorded at CARME, CQUET, and CLEJA stations, respectively. These stations are located on soil, rock, and soil profiles, respectively, and their respective epicentral distances are 13.02 km, 9.57 km, and 18 km. Fig. 8 shows the acceleration traces and corresponding 5 %-damped pseudo-accelerations spectra ( $PS_a$ ) of each component. As shown in the lowermost plots of the figure, the amplitude of the vertical  $PS_a$  changes substantially in

the period range between 0 and 0.5 s (or less), which corresponds to vertically rigid structures. This response is consistent with the acceleration histories for the vertical component of those records, in which high-frequency content is more noticeable than in the horizontal components. The plots also show that the vertical pseudo-acceleration can even exceed 1 g (Fig. 8a).

Fig. 9 presents the spectral  $V/H_{GM}$  ratio for the three motions. The spectral  $V/H_{GM}$  ratio was calculated for each motion by dividing the vertical  $PS_a$  spectrum over the geometric mean of the  $PS_a$

spectra of the horizontal components. By comparing the spectral  $V/H_{GM}$  ratios of the three motions with  $V/H = 2/3$ , it can be concluded that the recommendation in NSR-10 is too low for structures with vertical periods shorter than 0.25 s. These periods may correspond to the first vertical mode shapes of short-span bridges with simply-supported or continuous superstructures or the first vertical periods in most buildings [27]. Moreover, as occurred for event #29 at CLEJA station, the  $V/H_{GM}$  ratio can exceed 2/3 at periods longer than 1 s, which may be due to a local soft soil effect.

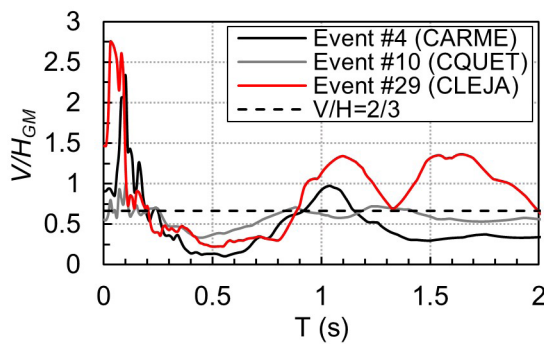
**Fig. 8.** Acceleration histories and pseudo-acceleration response spectra for the three components of records measured for events (a) #4 at CARME station, (b) #10 at CQUET station, and (c) #29 at CLEJA station.



Source: The authors.



**Fig. 9.** Spectral V/H ratios for the three example earthquake records.



**Source:** The authors.

## Conclusions

The main conclusions drawn from the results discussed in this paper are:

- 1) The peak ground acceleration of the vertical component ( $PGA_V$ ) of the Colombian earthquakes is, in general, smaller than that of the horizontal components. On average, the  $PGA_V$  is 0.6 times the  $PGA$  of the horizontal components. The vertical  $PGA$  increases as the epicentral distance decrease and can reach values ranging from 0.3g to 0.5g in sites closer to 20 km to the source during strong seismic events.
- 2) The  $PGA_V$  and the V/H ratios had a slightly stronger linear relationship with the hypocentral distance ( $R_{hypo}$ ) than to the epicentral distance or the moment magnitude ( $M_w$ ). However, the linear relationships were weak, indicating that non-linear prediction equations must be used to relate those parameters.
- 3) Simplified models were proposed to estimate the vertical  $PGA$  based on the dataset selected in this study. In the first model, the  $PGA_V$  is calculated as a function of an intercept,  $M_w$ , and  $R_{hypo}$ . The large variability of the data resulted in a determination coefficient ( $R^2$ ) of approximately 0.5 for this model. The other models provide relatively good estimations ( $R^2 \approx 0.8$ ) of the  $PGA_V$  as a function of  $PGA$  of each horizontal component or the geometric mean of the  $PGA$  of the horizontal components.

- 4) The V/H ratio equal to 2/3 suggested as a minimum in NSR-10 was found appropriate to estimate the  $PGA_V$ . This is supported by the results of the regression models mentioned above and by the fact that only 24% of the analyzed earthquake records showed V/H ratios larger than 2/3. Nonetheless, the NSR-10 recommendation is not acceptable to construct the entire vertical acceleration response spectrum based on the horizontal acceleration design spectrum. This is because the spectral V/H ratio changes substantially with the vertical stiffness of the structure (or its vertical period), and therefore a single value is not deemed appropriate. Further studies are required to develop functions of spectral V/H ratios that may be safer than the rule-of-thumb of  $V/H = 2/3$ .

## Acknowledgments

The authors thank the Vicerrectoría de Investigación y Extensión (VIE) at Universidad Industrial de Santander for the time provided to develop this investigation through Research Project FM2019-1. They also thank Luisa Castillo of the Servicio Geológico Colombiano (SGC) for providing the acceleration data of the seismic events while the SGC website underwent updates and for resolving the authors' inquiries promptly.

## References

- [1] J.-S. Jeon, A. Shafieezadeh, D. H. Lee, E. Choi, and R. DesRoches, "Damage assessment of older highway bridges subjected to three-dimensional ground motions: Characterization of shear-axial force interaction on seismic fragilities," *Engineering Structures*, vol. 87, pp. 47–57, March 2015. doi: <https://doi.org/10.1016/j.engstruct.2015.01.015>
- [2] F. Colangelo, "Effect of earthquake statistically correlated vertical component on inelastic demand to regular reinforced-concrete frames," *Engineering Structures*, vol. 211, p. 110492, May 2020. doi: <https://doi.org/10.1016/j.engstruct.2020.110492>
- [3] A. Papazoglou and A. Elnashai, "Analytical and Field Evidence of the Damaging Effect of Vertical Earthquake Ground Motion," *Earthquake Engineering & Structural Dynamics*, vol. 25, no. 10, pp. 1109–1137, October 1996. doi: [https://doi.org/10.1002/\(SICI\)1096-](https://doi.org/10.1002/(SICI)1096-)



- 9845(199610)25:10%3C1109::AID-EQE604%3E3.0.CO;2-0
- [4] J. Benjumea, M. Saiidi, and A. Itani, "Experimental and Analytical Seismic Studies of a Two-Span Bridge System with Precast Concrete Elements and ABC Connections," Center for Civil Engineering Earthquake Research, University of Nevada, Reno. Report No.: CCEER-19-02, Reno, United States, 2019.
- [5] A. Massumi and F. Gholami, "The influence of seismic intensity parameters on structural damage of RC buildings using principal components analysis," *Applied Mathematical Modelling*, vol. 40, no. 3, pp. 2161–2176, February 2016. doi: <https://doi.org/10.1016/j.apm.2015.09.043>
- [6] P. Ma, H. Wang, W. Jiang, and X. Zhang, "Research Status of Relationship between Seismic Instrument Intensity and Ground Motion Parameters," *IOP Conference Series Materials Science and Engineering*, vol. 780, no. 022002, pp. 1–8, April 2020. doi: <https://doi.org/10.1088/1757-899X/780/2/022002>
- [7] C. Collier and A. Elnashai, "A Procedure for Combining Vertical and Horizontal Seismic Action Effects," *Journal of Earthquake Engineering*, vol. 5, no. 4, pp. 521–539, October 2001. doi: <https://doi.org/10.1080/13632460109350404>
- [8] N. N. Ambraseys and K. A. Simpsom, "Prediction of Vertical Response Spectra in Europe," *Earthquake Engineering & Structural Dynamics*, vol. 25, no. 4, pp. 401–412, April 1996. doi: [https://doi.org/10.1002/\(SICI\)1096-9845\(199604\)25:4%3C401::AID-EQE551%3E3.0.CO;2-B](https://doi.org/10.1002/(SICI)1096-9845(199604)25:4%3C401::AID-EQE551%3E3.0.CO;2-B)
- [9] Y. Bozorgnia and K. Campbell, "The Vertical-to-Horizontal Response Spectral Ratio and Tentative Procedures for Developing Simplified V/H and Vertical Design Spectra," *Journal of Earthquake Engineering*, vol. 8, no. 2, pp. 175–207, 2004. doi: <https://doi.org/10.1080/13632460409350486>
- [10] S. Kim, C. Holub, and A. Elnashai, "Analytical Assessment of the Effect of Vertical Earthquake Motion on RC Bridge Piers," *Journal of Earthquake Engineering*, vol. 137, no. 2, pp. 252–260, February 2011. doi: [https://doi.org/10.1061/\(ASCE\)ST.1943-541X.0000306](https://doi.org/10.1061/(ASCE)ST.1943-541X.0000306)
- [11] AIS, Reglamento Colombiano de Construcción Sismo Resistente NSR-10. Bogotá D.C., Colombia: Asociación Colombiana de Ingeniería Sísmica (AIS), 2010.
- [12] AIS, Norma Colombiana de Diseño de Puentes - LRFD CCP14. Bogotá D.C., Colombia: Asociación Colombiana de Ingeniería Sísmica, AIS, 2014.
- [13] N. Newmark, J. Blume, and K. Kapur, "Seismic Design Spectra for Nuclear Power Plants," *Journal of the Power Division*, vol. 99, no. 2, pp. 287–303, November 1973. doi: <https://doi.org/10.1061/JPWEAM.0000753>
- [14] Servicio Geológico Colombiano, Visor Sismos. [Online]. Available: <https://www.sgc.gov.co/sismos>, accessed April 07, 2021.
- [15] Servicio Geológico Colombiano, Catálogo Aceleraciones. [Online]. Available: [http://bdrsn.sgc.gov.co/paginas1/catalogo/index\\_rnac.php](http://bdrsn.sgc.gov.co/paginas1/catalogo/index_rnac.php), accessed January 28, 2021.
- [16] A. S. Elnashai and L. Di Sarno, *Fundamentals of Earthquake Engineering*. New Jersey, United States: Wiley, 2008.
- [17] The MathWorks Inc., "MATLAB (R2020b)." 2020.
- [18] SEISMOSOFT - Earthquake Engineering Software Solutions, "SeismoSignal." 2021.
- [19] S. Kramer, *Geotechnical Earthquake Engineering: Pearson New International Edition*. United States: Pearson, 2014.
- [20] M. Fernández and J. Ardila, "Caracterización de la componente vertical de los sismos moderados y fuertes en Colombia," Undergrad tesis, Escuela de Ingeniería Civil, Universidad Industrial de Santander, Bucaramanga, Colombia, 2020.
- [21] A. Fernández, *Seismic Data Processing "SedPro"*. [Online]. Available: <https://la.mathworks.com/matlabcentral/fileexchange/95893-seismic-data-processing-sedpro>, accessed July 14, 2021.
- [22] K. W. Campbell and Y. Bozorgnia, "NGA Ground Motion Model for the Geometric Mean Horizontal Component of PGA, PGV, PGD and 5% Damped Linear Elastic Response Spectra for Periods Ranging from 0.01 to 10 s," *Earthquake Spectra*, vol. 24, no. 1, pp. 139–171, February 2008. doi: <https://doi.org/10.1193%2F1.2857546>
- [23] C. Adam, D. Kampenhuber, L. F. Ibarra, and S. Tsantaki, "Optimal Spectral Acceleration-based Intensity Measure for Seismic Collapse Assessment of P-Delta Vulnerable Frame Structures," *Journal of Earthquake Engineering*, vol. 21, no. 7, pp. 1189–1195, October 2017. doi: <https://doi.org/10.1080/13632469.2016.1210059>
- [24] R Core Team, "R: A Language and Environment for Statistical Computing." Vienna, Austria, 2020.
- [25] Peterson, B. G. and Carl, P., "PerformanceAnalytics: Econometric Tools for Performance and Risk Analysis," 2020. Available at: <https://cran.r-project.org/package=PerformanceAnalytics>.
- [26] Wickham, H. "ggplot2: Elegant Graphics for Data Analysis," 2016. Springer-Verlag New York. Available at: <https://ggplot2.tidyverse.org>.

- [27] C. Nayak, "A state-of-the-art review of vertical ground motion (VGM) characteristics, effects and provisions," *Innovative Infrastructure Solutions*, vol. 6, no. 2, p. 124, march, 2021. doi: <https://doi.org/10.1007/s41062-021-00491-3>

